AJNR

Noninvasive Follow-up Imaging of Ruptured Pediatric Brain AVMs Using Arterial Spin-Labeling

J.F. Hak, G. Boulouis, B. Kerleroux, S. Benichi, S. Stricker, F. Gariel, L. Garzelli, P. Meyer, M. Kossorotoff, N. Boddaert, N. Girard, V. Vidal, V. Dangouloff Ros, T. Blauwblomme and O. Naggara

AJNR Am J Neuroradiol 2022, 43 (9) 1363-1368
doi: https://doi.org/10.3174/ajnr.A7612
http://www.ajnr.org/content/43/9/1363

Noninvasive Follow-up Imaging of Ruptured Pediatric Brain AVMs Using Arterial Spin-Labeling

J.F. Hak, G. Boulouis, B. Kerleroux, S. Benichi, S. Stricker, F. Gariel, L. Garzelli, P. Meyer, M. Kossorotoff, N. Boddaert, N. Girard, V. Vidal, V. Dangouloff Ros, T. Blauwblomme, and O. Naggara

ABSTRACT

BACKGROUND AND PURPOSE: Brain AVMs represent the main etiology of pediatric intracranial hemorrhage. Noninvasive imaging techniques to monitor the treatment effect of brain AVMs remain an unmet need. In a large cohort of pediatric ruptured brain AVMs, we aimed to investigate the role of arterial spin-labeling for the longitudinal follow-up during treatment and after complete obliteration by analyzing CBF variations across treatment sessions.

MATERIALS AND METHODS: Consecutive patients with ruptured brain AVMs referred to a pediatric quaternary care center were prospectively included in a registry that was retrospectively queried for children treated between 2011 and 2019 with unimodal or multimodal treatment (surgery, radiosurgery, embolization). We included children who underwent an arterial spin-labeling sequence before and after treatment and a follow-up DSA. CBF variations were analyzed in univariable analyses.

RESULTS: Fifty-nine children with 105 distinct treatment sessions were included. The median CBF variation after treatment was −43 mL/100 mg/min (interquartile range, −102−5.5), significantly lower after complete nidal surgical resection. Following radiosurgery, patients who were healed on the last DSA follow-up demonstrated a greater CBF decrease on intercurrent MR imaging, compared with patients with a persisting shunt at last follow-up (mean, −62 [SD, 61] mL/100 mg/min versus −17 [SD, 40.1] mL/100 mg/min; $P = .02$). In children with obliterated AVMs, recurrences occurred in 12% and resulted in a constant increase in CBF (mean, +89 [SD, 77] mL/100 mg/min).

CONCLUSIONS: Our results contribute data on the role of noninvasive arterial spin-labeling monitoring of the response to treatment or follow-up after obliteration of pediatric AVMs. Future research may help to better delineate how arterial spin-labeling can assist in decisions regarding the optimal timing for DSA.

ABBREVIATIONS: ASL = arterial spin-labeling; EVT = endovascular treatment; IQR = interquartile range; SRS = stereotactic radiosurgery

Pediatric intracerebral hemorrhage accounts for half of strokes in children[1-3] and has severe long-term medical and psychosocial consequences.[4] In children, brain AVMs represent the main underlying risk factor for hemorrhage, being responsible for up to 80% of nontraumatic hemorrhages.[1,3] Treatment strategy includes surgical excision, serial endovascular treatment (EVT), and stereotactic radiosurgery (SRS), alone or in combination, according to the AVM size and location. After the initial work-up and treatment of a ruptured AVM, invasive DSA is the criterion standard to tailor the adequate subsequent therapeutic strategy[5,6] or to confirm the complete obliteration of the AVM. Nevertheless, repeat DSA exposes children to the long-term risks of ionizing radiation, injection of an exogenous contrast agent, multiple exposures to general anesthesia, and neurologic adverse events. Hence, in children with ruptured AVMs, evaluating noninvasive imaging techniques for the mid and long-term intermediate follow-up and treatment

Received February 2, 2022; accepted after revision June 28.

From the Department of Pediatric Radiology (J.F.H., G.B., B.K., F.G., L.G., N.B., V.D.R., O.N.), Pediatric Neurointensive Care Unit (P.M.), and Department of Pediatric Neurology (M.K.), Assistance Publique–Hôpitaux de Paris, Hôpital Universitaire, Necker Hospital–Sick Children, Paris, France; Department of Neuroradiology (J.F.H., G.B., B.K., O.N.), GHU Paris, Paris, France; L'Institut National de la Santé et de la Recherche Médicale, University Hospital Group Paris, 1266, IMA-BRAIN (J.F.H., G.B., B.K., O.N.), Université de Paris, Paris, France; Department of Pediatric Neurosurgery (S.B., S.S., T.B.), Institut Imagine, L'Institut National de la Santé et de la Recherche Médicale, Unité Mixte de Recherche 1163, Assistance Publique–Hôpitaux de Paris, Necker Hospital–Sick Children, Paris, France; Department of Neuroradiology (F.G.), University Hospital of Bordeaux, Bordeaux, France; INSERM U894, French Center for Pediatric Stroke (M.K., T.B., O.N.), L'Institut National de la Santé et de la Recherche Médicale, Paris, France; Departments of Neuroradiology (N.G.) and Radiology (V.V.), University Hospital La Timone Hospital, Assistance Publique–Hôpitaux de Marseille, Marseille, France; Université de Paris (N.B., V.D.R.), L'Institut National de la Santé et de la Recherche Médicale, ERL, Paris, France; and Institut Imagine (N.B., V.D.R.), Université de Paris, Unité Mixte de Recherche 1163, Paris, France.

J.F. Hak and G. Boulouis contributed equally to this work.

J.F. Hak was supported by a grant provided by the Société Française de Radiologie, French Society of Radiology, together with the Collège des Enseignants en Radiologie de France, French Academic College of Radiology.

Please address correspondence to Jean-Francois Hak, MD, Department of Pediatric Radiology, AP-HP, University Hospital Necker-Enfants-Malades, 75015 Paris, France; e-mail: jeanfrancois.hak@gmail.com; @JFHak

http://dx.doi.org/10.3174/ajnr.A7612

planning is an important purpose. In this context, MR imaging possibly represents the best noninvasive technique, and advanced techniques such as arterial spin-labeling (ASL) sequences have shown their role in detecting increased CBF in patients with AVMs[6] and are useful tools in adults for the follow-up of AVMs after embolization[7] or SRS.[8-11] Furthermore, accumulating evidence indicates that AVMs in children are more likely to re-appear after DSA-proved complete obliteration,[12,13] reinforcing the need for prolonged follow-up and the drawbacks of invasive imaging in the setting of a healed shunt. A preliminary analysis from our group[14] evaluated the CBF, computed using ASL after treatment in 21 patients (yet only including 9 patients who had undergone ASL both before and after therapeutic procedures), and demonstrated its potential role in the noninvasive follow-up of AVMs in patients under treatment or after treatment.

In a large cohort of children with an initially ruptured AVM, we aimed to investigate the role of ASL for the longitudinal follow-up of patients under treatment and after complete obliteration by analyzing CBF variations on pseudocontinuous ASL across treatment sessions.

MATERIALS AND METHODS

Study Design and Patient Selection

Consecutive patients referred to our institution, a pediatric quaternary care center and coordinating center for the French Pediatric Stroke Network, were prospectively enrolled in a registry initiated in 2008. The registry has been described elsewhere in detail.[4] For the purpose of this analysis, the sample was restricted to children (1 month to 18 years of age) meeting the following criteria: 1) ruptured brain AVMs; 2) between January 2011 (date of ASL implementation at our site) and October 2019; 3) with unimodal or multimodal AVM treatment (surgery, SRS, embolization); and 4) an ASL sequence before and after treatment and intercurrent DSA, performed within 24 hours of the ASL sequence. Patients were excluded for the following reasons: 1) no ASL follow-up; 2) no DSA follow-up; 3) a ruptured AVM without treatment; and 4) lost to follow-up.

Imaging Acquisition

MR Imaging Procedure. MR imaging was performed for each patient with a Signa HDxt 1.5T system (GE Healthcare) and a 12-channel head-neck-spine coil. The MR imaging investigation included standard pulse sequences according to local AVM protocol: 3D T1WI, 4D-MRA, gadolinium-enhanced 3D T1WI, T2*WI, DWI, TOF-MRA of the circle of Willis, and unenhanced perfusion imaging with a 3D pseudocontinuous ASL sequence. Acquisition parameters for the ASL pulse sequence were unchanged since the beginning of the protocol:[14] TR/TE, 4428/10.5 ms; postlabeling delay, 1025 ms; label duration, 1500 ms; 80 axial partitions; FOV, 240 × 240 × 4 mm; acquisition matrix, 8 spiral arms in each 3D partition with 512 points per arm; flip angle, 155°; acquisition time, 4 minutes 17 seconds.

Paired DSA and ASL. At our institution, follow-up DSAs are performed 3 years after SRS or after the last treatment to document AVM obliteration, 3 and 5 years thereafter, and at 18 years of age, whichever comes last. DSAs were performed with the patient under general anesthesia in a dedicated neuroangiography suite. A brain MR imaging including an ASL sequence was performed systematically the day before DSA.

Imaging Analysis

DSA Analysis. Two readers (15 [O.N.] and 7 [G.B.] years of experience) evaluated DSA during a single joint reading session. A residual AVM was defined as the early opacification of a cerebral vein, visible in the vicinity of nidal location, during the arterial phase of angiographic runs.

MR Imaging and ASL Analysis. Image analysis was performed using a PACS, independently, by 2 readers (6 [J.F.H.] and 5 [B.K.] years of experience). Readers were blinded to clinical and follow-up data and reported patient and AVMs characteristics. The CBF map was automatically generated using the 3D-ASL application of the Advantage Windows Workstation Functool (GE Healthcare) postprocessing software. For qualitative analysis, the color scale was set to rainbow with the warmer color representing the highest CBF.

Criteria for the presence of an AVM on MR images were defined with the visualization of an early venous filling at the arterial phase (4D-MRA), enlarged and dilated serpiginous vessels (TOF-MRA, postgadolinium 3D-T1), and/or direct visualization of the fistulous point/nidus (TOF-MRA)[15] and, for ASL, the presence of an intracranial venous hypersignal within the dural sinuses or cortical veins and a focal intravascular warm color ("hot spot") on a CBF map.

The quantitative analysis of ASL was staged as follows:

1. Visual inspection of the ASL-derived CBF maps and identification of the most densely perfused areas of the lesion, if present.
2. 2D ROI placement using a calibrated round 20-mm^2 ROI on the region where the CBF was visually of the highest value corresponding to the AVM nidus or draining vein. Inside each ROI, the nidus CBF (CBF_{nidus}) mean values were automatically calculated by the software. We analyzed the mean values of the 2 readers for each variable. For each patient, the ROI was placed in the exact same hot spot localization as in the MRIs performed before and after each treatment.
3. The relative lesion CBF, corresponding to the ratio of CBF_{nidus}/CBF_{cortex}, was obtained by normalizing CBF to a 20-mm^2 ROI in the contralateral normal-appearing cortical gray matter (CBF_{cortex}) in the cerebellum for posterior fossa AVMs and in the frontal and parietal lobes for supratentorial AVMs. Gray matter was chosen as a reference because it has a higher SNR.

If a difference of >10 mL/100 mg/min was realized between the 2 readers, a consensus was reached on CBF maps and other MR imaging sequences to best position the ROIs. In case of negative ASL findings following treatment, the nidus ROI was placed at the exact same localization as the presurgical ASL ROI after manual coregistration of MR imaging sequences.

Statistical Analysis

Baseline characteristics were explored using descriptive statistics as appropriate per variable makeup and are displayed as absolute number (percentage) or mean (SD) or median (interquartile

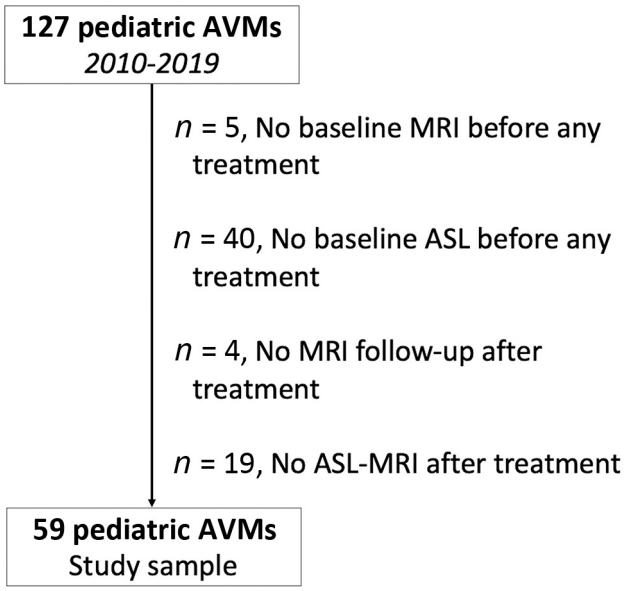

FIG 1. Flow chart of patient selection.

range [IQR], eg, 25th–75th quantiles). Univariable comparisons were performed using appropriate tests per variable makeup, distribution, and central tendency. All analyses were performed using JMP, Version Pro 14 (SAS Institute; 1989–2019), with $P < .05$ as a threshold for statistical significance.

RESULTS

Patients and AVM Characteristics

A total of 127 children were prospectively enrolled after 2011 in the database. After the application of study-specific inclusion and exclusion criteria, 59 patients were analyzed, and 68 patients were excluded. The flow chart in Fig 1 details patient selection. In included patients, AVMs were more frequently superficially located (57.4% versus 29.3%, $P = .02$). There was no difference between included and excluded patients in age at presentation (mean, 9.8 [SD, 3.7] versus 9.8 [SD, 3.8] years), clinical outcomes ($P = .36$), AVM location (supratentorial, 90% versus 83%, $P = .23$), and AVM grades ($P = .12$).

The 59 included patients benefited from 105 distinct treatment sessions with pre- and posttreatment MR imaging including ASL. The initial treatment was partial EVT, SRS, and partial and exhaustive microsurgery for, respectively, 38 (64.4%), 12 (20.3%), 3 (5.1%), and 6 (10.2%) children. Study sample baseline characteristics as well as treatments are detailed in the Table.

On baseline MR imaging performed before any treatment, findings of the visual inspection of the ASL-derived CBF map were considered positive in 56 patients (94.9%). The mean CBF_{nidus} was 192.1 (SD, 106) mL/100 mg/min with a mean ratio of lesion/cortex CBF of 2.2 (SD, 1.2).

AVM Follow-up of Patients under Treatment

General Considerations. We observed high interreader agreement for CBF measurement, using the Fleiss κ analysis ($\kappa = 0.92$; 95% CI, 0.8–1.0; $P < .0001$). The median CBF variation after treatment was −43 mL/100 mg/min (IQR, −102−5.5 mL/100 mg/min). There was a higher decrease in CBF after exhaustive nidal microsurgery ($n = 13$; median, −98 mL/100 mg/min [IQR, −161 to −50]) than after EVT, SRS, or partial microsurgery ($P = .002$). There was no significant difference in CBF variations after EVT versus SRS, SRS versus partial microsurgery, or EVT versus partial microsurgery (all $P > .05$) (see Fig 2 for details). The median time interval between MR imaging examinations was 10 months (IQR, 4–20 months).

Patient characteristics[a]

Characteristics	
Clinical presentation	
Male sex (%)	28 (47.5%)
Age (median) (IQR) (yr)	10.1 (7.2–13.0)
Headaches	50 (84.7%)
Seizures	15 (25.4%)
Emesis	37 (62.7%)
Focal deficit	22 (37.3%)
GCS (median) (IQR)	14 (3–15)
ICH characteristics	
Supratentorial location	41 (69.5%)
ICH volume (median) (IQR) (mL)	10.9 (0.1–58)
ICH/TBV (median) (IQR) (%)	1.2 (0.8–5.6)
IVH	8 (13.6%)
Treatment characteristics	
Total No. of treatments	105
Patients treated with unimodal treatment	38 (64.4%)
Patients treated with multimodal treatment	21 (35.6%)
No. of treatment sessions (median) (IQR)	1 (1–6)
EVT	58 (55.2%)
EVT (No. of sessions) (median) (IQR)	1.5 (1–5)
SRS	26 (24.8%)
Partial surgery	6 (5.7%)
Complete surgery	15 (14.3%)
AVM characteristics	
Brain AVM	59 (100%)
SM grade 1–2	38 (64.4%)
SM grade 3	14 (23.7%)
SM grade 4–5	7 (11.9%)
Supratentorial	49 (83%)
Deep	31 (52.5%)
Eloquent area	33 (55.9%)
Nidus size (median) (IQR) (mm)	22 (9–60)
Compact nidus	38 (64.4%)
Aneurysm (arterial/venous)	25 (42.4%)
Any deep venous drainage	30 (50.8%)

Note:—GCS, indicates Glasgow Coma Scale; ICH, intracerebral hemorrhage; TBV, total brain volume; IVH, intraventricular hemorrhage; SM, Spetzler-Martin.
[a] Variables are displayed as No. (%) or median (25th to 75th quantiles).

CBF Variation after SRS. Twenty-seven patients were treated with SRS, and an ASL sequence was performed before and after treatment at each SRS session. The median interval time delay between sessions of MR imaging was 26 months (IQR, 12–39.5 months). Among these patients, DSA-proved complete obliteration at last follow-up was found in 14 patients (51.9%), whereas 13 patients were still under surveillance. The mean variation in CBF values on interval MRIs was −62 (SD, 61) mL/100 mg/min in eventually healed patients, whereas it was −17 (SD, 40.1) mL/100 mg/min in patients with incomplete obliteration at last follow-up ($P = .02$). In 8 of the 27 patients treated with SRS, CBF did not decrease ($\Delta > 0$), and only 2/8 (25%) of these patients' AVMs were obliterated at the latest follow-up.

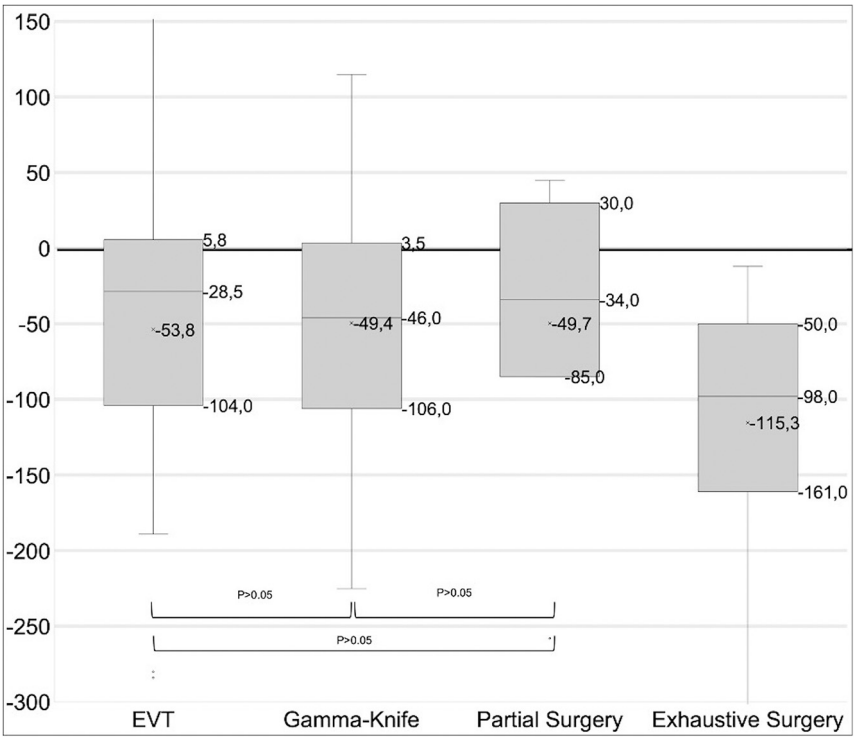

FIG 2. Boxplots of ASL variations by treatment technique per time interval.

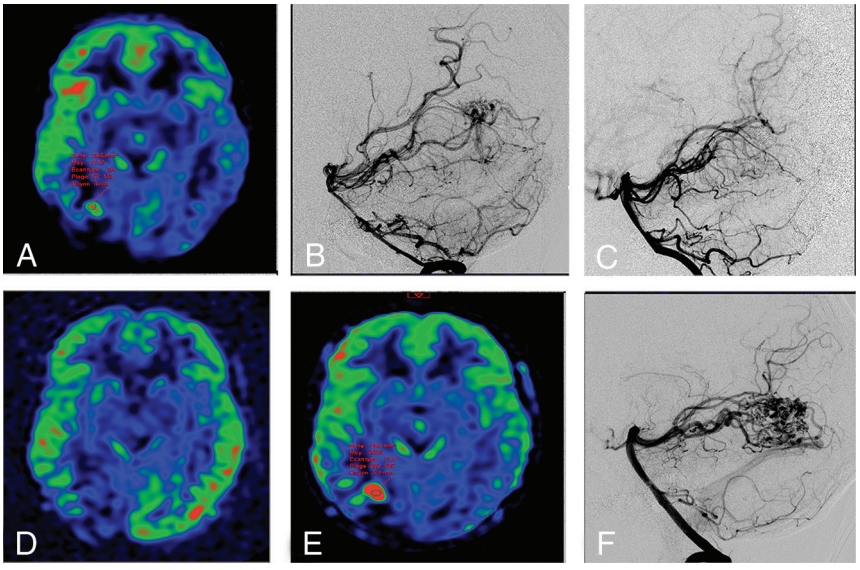

FIG 3. Example of a right occipital ruptured AVM confirmed with ASL (*A*) and DSA (*B*), completely treated with embolization 15 days after the initial diagnosis (*C*) and without a CBF increase, with ASL performed 4 months after the initial diagnosis (*D*). The 4-year ASL control revealed a focal ASL-derived CBF increase (*E*) suspicious for recurrence, confirmed with DSA (*F*).

After SRS, the mean CBF Δ for the healed children at 3 years versus the nonhealed at 3 years was, respectively, −68.3 (SD, 61.0) ($n = 4$) versus −14.5 (SD, 17.7) ($n = 2$) at 1 year after SRS ($n = 6$), and, respectively, −105.8 (SD, 66.3) versus 65.7 (SD, 150.3) at 2 years after SRS ($n = 19$). Thus, 1 year after SRS, a decrease in CBF of > 50mL/100 mg/min was associated with a 3-fold increase in the rate of eventual obliteration after 3 years.

Follow-up after Complete Obliteration. Among 34 patients achieving DSA-proved complete obliteration during follow-up, 4 (11.8%) children presented with a DSA recurrence at a mean delay of 21.8 [SD, 22.2] months. At the time of recurrence, the CBF increased in all patients by a mean of 89 (SD, 77) mL/100 mg/min, corresponding to relative CBF lesion increases of a mean of 311% (SD, 147%). See Fig 3 for an example of recurrence after treatment.

DISCUSSION

We present robust data on the role of ASL in the noninvasive follow-up of ruptured pediatric AVMs during and after treatment. Our analysis notably shows that ASL-CBF increased in all patients with DSA recurrences, with direct clinical applications in children followed up after AVM obliteration. Furthermore, we showed that 1 year after SRS, a decrease in CBF of > 50mL/100 mg/min was associated with a 3-fold increase in the rate of eventual obliteration after 3 years. In our sample, patients with eventually healed AVMs after SRS had a mean CBF decrease of –62 mL/100 mg/min when it was −17 mL/100 mg/min in patients with incomplete obliteration at 3 years.

These results add to the evidence of the role of noninvasive imaging in objectively delineating treatment effect in pediatric AVMs, provide additional evidence justifying intermediate MR imaging follow-up of children with obliterated AVMs, and pave the way for noninvasive biomarkers of anticipated treatment effect, especially after SRS. An additional supporting argument was the high interreader agreement for CBF measurement, suggesting the reproducibility of our findings, at least internally.

Several adult studies reported a role for ASL in AVM follow-up after treatment. Suazo et al[7] reported a fair agreement between ASL and DSA for the assessment of shunt reduction achieved by embolization for 8 AVMs. Other studies focusing on SRS-treated AVMs reported a promising role for ASL: first, to show and quantify differences in AVM nidal flow ratios and the associated steal phenomena between treated and untreated groups;[16] and second, to detect

incomplete-versus-complete AVM obliteration.[8-11] Altogether, these results contribute to determining the important role of ASL in AVM follow-up for patients under treatment or after obliteration, to minimize the use of DSA in the vulnerable sample of children with ruptured AVMs.

Pediatric AVMs have been shown to be dynamic lesions with vascular changes and higher rates of recurrence after complete obliteration, compared with adults.[12,13] In addition, the susceptibility effects of the liquid embolic agents on perfusion imaging may hinder the quantitative perfusion measurements,[17] justifying the need for our analysis in the subgroup of ruptured pediatric AVMs. This analysis complements a preliminary work from our group,[14] in which 3 ruptured pediatric AVMs followed up after embolization alone showed a reduction in both nidus size and ASL-derived CBF values as well as 5 ruptured pediatric AVMs followed up after SRS, in which a reduction in the nidus size was observed, despite persistent elevated CBF_{nidus} values.

Despite these prior data, noninvasive AVM follow-up is an unmet need. Studies have evaluated 4D-MRA for AVM follow-up, but there are many practical drawbacks to the use of IV contrast in pediatric patients, including the need for IV access; increased scan time; children's fatigue, anxiety, and motion; and exposure to possible adverse effects of the contrast agent.[18-23] Conversely, ASL sequences allow quantitative mapping of CBF, without contrast injection,[24] and are known to be relevant in detecting the presence of arteriovenous shunts by demonstrating high signal in the nidus as well as arterialized venous structures.[14,25-27]

In line with previous studies,[7-11,16,28] we showed that most patients had decreased CBF after treatment with SRS or embolization, yet some lesions demonstrated no CBF decrease despite interval treatment. This finding supports the concept of dynamic AVM lesions in children, considered as an evolving vasculopathy rather than a simple amorphous vascular connection, with interval increasing arterial feeding and/or shunt acceleration. It appears, therefore, that AVMs have a remodeling potential that explains the reported cases of spontaneous growth [29,30] as well as spontaneous regression.[31-33] Therefore, pretreatment ASL allows a radiation- and injection-free tool for treatment planning.

As previously reported, the AVM recurrence rate is higher for pediatric AVMs than for those in adults.[12,13] In our cohort, 4 (11.8%) children presented with an angiographic recurrence with a CBF increase in all patients, by a mean of 89 (SD, 77) mL/100 mg/min. To our knowledge, we report the first preliminary data on ASL-CBF increase for the diagnosis of recurrent AVMs. We acknowledge, nonetheless, that our sample provides a limited number of recurrent AVMs and that this finding should be further supported by a larger study.

Note that at our institution, a pediatric quaternary care center and coordinating center for the French Pediatric Stroke Network, a DSA is performed in the initial AVM imaging assessment for angioarchitectural characterization and appropriate treatment. Following treatment, DSAs are performed 3 years after SRS or after the last treatment to document AVM obliteration, 3 and 5 years thereafter, and at 18 years of age, whichever comes last. Accordingly, DSA is not replaced by ASL, but ASL should be considered as a tool to facilitate the timing of follow-up DSA studies, reduce the number of DSAs for each patient, and for the planning of additional AVM treatment.

Our study has several shortcomings, mostly inherent in its retrospective and noncontrolled design. Specifically, in our center, to optimize the SNR of the ASL sequence for AVMs detection,[34] we used a postlabeling delay of 1025 ms, shorter than the value typically recommended (1500 ms).[35] We chose this postlabeling because we have been using it since 2011, after local optimization with an excellent SNR across various cerebrovascular diseases. Second, this approach is very commonly used by experienced teams using ASL and has been validated extensively.[36]

We also acknowledge that some patients have been lost to imaging follow-up following SRS outside our center, introducing some degree of attrition bias. Finally, these results were obtained in a sample of ruptured brain AVMs and may not be transferrable to children with initially unruptured lesions.

CONCLUSIONS

In children with ruptured AVMs, ASL allows detection of hemodynamic changes after treatment, noninvasively and without radiation exposure or contrast media administration. Our results contribute data on the role of noninvasive ASL monitoring of the response of pediatric AVMs to treatment or follow-up after obliteration. Future research may help better elucidate how ASL can assist in decisions regarding optimal timing for DSA.

Disclosure forms provided by the authors are available with the full text and PDF of this article at www.ajnr.org.

REFERENCES

1. Boulouis G, Blauwblomme T, Hak JF, et al. **Nontraumatic pediatric intracerebral hemorrhage.** *Stroke* 2019;50:3654–61 CrossRef Medline
2. Beslow LA, Licht DJ, Smith SE, et al. **Predictors of outcome in childhood intracerebral hemorrhage: a prospective consecutive cohort study.** *Stroke* 2010;41:313–18 CrossRef Medline
3. Boulouis G, Stricker S, Benichi S, et al. **Etiology of intracerebral hemorrhage in children: cohort study, systematic review, and meta-analysis.** *J Neurosurg Pediatr* 2021;27:357–63 CrossRef Medline
4. Guédon A, Blauwblomme T, Boulouis G, et al. **Predictors of outcome in patients with pediatric intracerebral hemorrhage: development and validation of a modified score.** *Radiology* 2018;286:651–58 CrossRef Medline
5. Ferriero DM, Fullerton HJ, Bernard TJ, et al; American Heart Association Stroke Council and Council on Cardiovascular and Stroke Nursing. **Management of stroke in neonates and children: a scientific statement from the American Heart Association/American Stroke Association.** *Stroke* 2019;50:e51–96 CrossRef Medline
6. Ziyeh S, Strecker R, Berlis A, et al. **Dynamic 3D MR angiography of intra- and extracranial vascular malformations at 3T: a technical note.** *AJNR Am J Neuroradiol* 2005;26:630–04 Medline
7. Suazo L, Foerster B, Fermin R, et al. **Measurement of blood flow in arteriovenous malformations before and after embolization using arterial spin-labeling.** *Interv Neuroradiol* 2012;18:42–48 CrossRef Medline
8. Amponsah K, Ellis TL, Chan MD, et al. **Retrospective analysis of imaging techniques for treatment planning and monitoring of obliteration for gamma knife treatment of cerebral arteriovenous malformation.** *Neurosurgery* 2012;71:893–900 CrossRef Medline
9. Heit JJ, Thakur NH, Iv M, et al. **Arterial-spin labeling MRI identifies residual cerebral arteriovenous malformation following stereotactic radiosurgery treatment.** *J Neuroradiol* 2020;47:13–19 CrossRef Medline
10. Kodera T, Arai Y, Arishima H, et al. **Evaluation of obliteration of arteriovenous malformations after stereotactic radiosurgery with arterial**

spin-labeling MR imaging. *Br J Neurosurg* 2017;31:641–47 CrossRef Medline
11. Shimizu K, Kosaka N, Yamamoto T, et al. **Arterial spin-labeling perfusion-weighted MRI for long-term follow-up of a cerebral arteriovenous malformation after stereotactic radiosurgery.** *Acta Radiol Short Rep* 2014;3:2047981613510160 CrossRef Medline
12. Copelan A, Drocton G, Caton MT, et al; UCSF Center For Cerebrovascular Research and UCSF Pediatric Brain Center. **Brain arteriovenous malformation recurrence after apparent microsurgical cure: increased risk in children who present with arteriovenous malformation rupture.** *Stroke* 2020;51:2990–96 CrossRef Medline
13. Sorenson TJ, Brinjikji W, Bortolotti C, et al. **Recurrent brain arteriovenous malformations (AVMs): a systematic review.** *World Neurosurg* 2018;116:e856–66 CrossRef Medline
14. Blauwblomme T, Naggara O, Brunelle F, et al. **Arterial spin-labeling magnetic resonance imaging: toward noninvasive diagnosis and follow-up of pediatric brain arteriovenous malformations.** *J Neurosurg Pediatr* 2015;15:451–58 CrossRef Medline
15. Sporns PB, Psychogios M-N, Fullerton HJ, et al. **Neuroimaging of pediatric intracerebral hemorrhage.** *J Clin Med* 2020;9:1518 CrossRef Medline
16. Pollock JM, Whitlow CT, Simonds J, et al. **Response of arteriovenous malformations to gamma knife therapy evaluated with pulsed arterial spin-labeling MRI perfusion.** *AJR Am J Roentgenol* 2011;196:15–22 CrossRef Medline
17. Deibler AR, Pollock JM, Kraft RA, et al. **Arterial spin-labeling in routine clinical practice, Part 1: technique and artifacts.** *AJNR Am J Neuroradiol* 2008;29:1228–34 CrossRef Medline
18. Dillman JR, Ellis JH, Cohan RH, et al. **Frequency and severity of acute allergic-like reactions to gadolinium-containing IV contrast media in children and adults.** *AJR Am J Roentgenol* 2007;189:1533–38 CrossRef Medline
19. Auron A, Shao L, Warady BA. **Nephrogenic fibrosing dermopathy in children.** *Pediatr Nephrol* 2006;21:1307–11 CrossRef Medline
20. Foss C, Smith JK, Ortiz L, et al. **Gadolinium-associated nephrogenic systemic fibrosis in a 9-year-old boy.** *Pediatr Dermatol* 2009;26:579–82 CrossRef Medline
21. Hu HH, Pokorney A, Towbin RB, et al. **Increased signal intensities in the dentate nucleus and globus pallidus on unenhanced T1-weighted images: evidence in children undergoing multiple gadolinium MRI exams.** *Pediatr Radiol* 2016;46:1590–98 CrossRef Medline
22. Nguyen NC, Molnar TT, Cummin LG, et al. **Dentate nucleus signal intensity increases following repeated gadobenate dimeglumine administrations: a retrospective analysis.** *Radiology* 2020;296:122–30 CrossRef Medline
23. Flood TF, Stence NV, Maloney JA, et al. **Pediatric brain: repeated exposure to linear gadolinium-based contrast material is associated with increased signal intensity at unenhanced T1-weighted MR imaging.** *Radiology* 2017;282:222–28 CrossRef Medline
24. Detre JA, Rao H, Wang DJJ, et al. **Applications of arterial spin-labeled MRI in the brain.** *J Magn Reson Imaging* 2012;35:1026–37 CrossRef Medline
25. Wolf RL, Wang J, Detre JA, et al. **Arteriovenous shunt visualization in arteriovenous malformations with arterial spin-labeling MR imaging.** *AJNR Am J Neuroradiol* 2008;29:681–87 CrossRef Medline
26. Iryo Y, Hirai T, Kai Y, et al. **Intracranial dural arteriovenous fistulas: evaluation with 3-T four-dimensional MR angiography using arterial spin labeling.** *Radiology* 2014;271:193–99 CrossRef Medline
27. Le TT, Fischbein NJ, André JB, et al. **Identification of venous signal on arterial spin labeling improves diagnosis of dural arteriovenous fistulas and small arteriovenous malformations.** *AJNR Am J Neuroradiol* 2012;33:61–68 CrossRef Medline
28. Schubert T, Clark Z, Sandoval-Garcia C, et al. **Non contrast, pseudo-continuous arterial spin-labeling and accelerated 3-dimensional radial acquisition intracranial 3-dimensional magnetic resonance angiography for the detection and classification of intracranial arteriovenous shunts.** *Invest Radiol* 2018;53:80–86 CrossRef Medline
29. Mendelow AD, Erfurth A, Grossart K, et al. **Do cerebral arteriovenous malformations increase in size?** *J Neurol Neurosurg Psychiatry* 1987;50:980–87 CrossRef Medline
30. Waltimo O. **The change in size of intracranial arteriovenous malformations.** *J Neurol Sci* 1973;19:21–27 Medline
31. Lee SK, Vilela P, Willinsky R, et al. **Spontaneous regression of cerebral arteriovenous malformations: clinical and angiographic analysis with review of the literature.** *Neuroradiology* 2002;44:11–16 CrossRef Medline
32. Nukui H, Miyagi O, Tamada J, et al. **Long-term follow-up study by cerebral angiography in cases with arteriovenous malformation of the brain: with special reference to spontaneous disappearance of arteriovenous malformation in cerebral angiography (author's transl)** [in Japanese]. *Neurol Med Chir (Tokyo)* 1982;22:125–32 CrossRef Medline
33. Sawlani V, Handique A, Phadke RV. **Spontaneous regression of cerebral AVM due to thrombosis of draining vein: angiographic and MRI demonstration.** *J Neurol Sci* 2004;223:195–98 CrossRef Medline
34. Lüdemann L, Jedrzejewski G, Heidenreich J, et al. **Perfusion imaging of cerebral arteriovenous malformations: a study comparing quantitative continuous arterial spin labeling and dynamic contrast-enhanced magnetic resonance imaging at 3 T.** *Magn Reson Imaging* 2011;29:1157–64 CrossRef Medline
35. Alsop DC, Detre JA, Golay X, et al. **Recommended implementation of arterial spin-labeled perfusion MRI for clinical applications: a consensus of the ISMRM perfusion study group and the European Consortium for ASL in Dementia.** *Magn Reson Med* 2015;73:102–16 CrossRef Medline
36. Jain V, Duda J, Avants B, et al. **Longitudinal reproducibility and accuracy of pseudo-continuous arterial spin–labeled perfusion MR imaging in typically developing children.** *Radiology* 2012;263:527–36 CrossRef Medline